19th Australasian Fluid Mechanics Conference
Melbourne, Australia
8-11 December 2014

Design of Test Flows to Investigate Binary Scaling in High Enthalpy $CO_2 - N_2$ Mixtures

G. de Crombrugghe[1], D. Gildfind[1], F. Zander[2], T. McIntyre[1], and R. Morgan[1]

[1]Centre for Hypersonics
University of Queensland, Brisbane 4072, Australia
[2]Institut für Raumfahrtsysteme
Universität Stuttgart, Stuttgart 70569, Germany

Abstract

Binary scaling is a similitude law that facilitates the study of hypersonic flows around blunt bodies. It conserves the Reynolds number and the binary (two-body) reaction rates, which are mainly present in the nonequilibrium layer, and scales properly the convective heat transfer. It requires duplication of the product of density and a length scale of the flow, ρL, as well as the free-stream enthalpy, H_∞^{tot}. Its use for ground-to-flight extrapolation depends on the fractional extent of regions of the flow where higher order reactions become important.

This paper presents the design of flow conditions relevant to the study of binary scaling for the X2 super-orbital expansion tube. Flows conditions with similar free-stream enthalpy but distinct free-stream densities were obtained. With the help of numerical simulation, it was confirmed that those conditions were suitable to isolate the effect of binary scaling from the uncertainties and scattering of free-stream conditions.

Binary Scaling

State of the Art

The binary scaling law, originally suggested by Birkhoff [1], aims to achieve proper duplication of chemically reacting hypersonic flows dominated by binary (two-body) reactions. It is known to be useful for creating partial similarity between laboratory flow and hypersonic flight. Despite its known limitations, it is commonly used as a scaling parameter [9, 12].

In shock layers, binary reactions dominate the nonequilibrium region immediately downstream of the shock, as depicted in figure 1. Further away from the shock, the flow reaches its equilibrium state through a series of ternary (three-body) reactions. Gibson noted that duplication through binary scaling would be correct at sufficiently high altitude (i.e. large Knudsen number), where a large portion the shock layer is expected to be in nonequilibrium [4]. This has been verified by Hall et al. with numerical correlations for inviscid flows [8]. They further demonstrated the applicability of binary scaling to vibrational and electronic relaxation processes, thereby ensuring scaling of shock layer radiation [8]. Gibson and Marrone then developed an analytical method to determine the chemical composition of shock layers around hypersonic blunt bodies [5]. Based on that method, they drew limits in terms of altitude, nose radius and velocity for which the shock layer is mostly in nonequilibrium, and binary scaling is thus applicable [5]. Ellington later suggested a refined method to take the interdependence of those limits into account [2]. However useful they are, they exclude most of the flow regimes for which radiative heating is a significant contribution to the total heating. Furthermore, although some aspects of radiating flows can be reproduced with the binary scaling, it does not capture the coupling that can exist between the radiation and the gas dynamics.

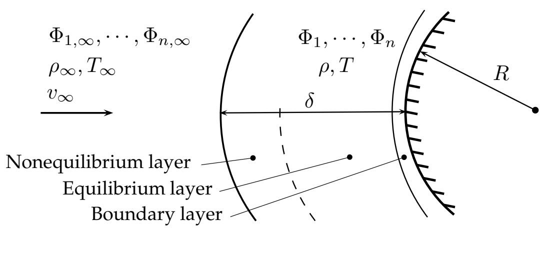

Figure 1: Schematic representation of the regions and parameters of interest in the vicinity of the stagnation line of a hypersonic blunt body flow.

Derivation

Across the normal shock in front of a blunt body, most of the flow kinetic energy is transferred into thermal energy, resulting in very high post-shock temperatures. In order to account for the gas chemistry, the mass balance equation has to be solved for every species simultaneously. In steady-state, it becomes:

$$\partial \left(\rho v_i + J_i\right) / \partial x_i = \dot{w} \quad (1)$$

where Einstein's notation is used. The subscript i denotes a direction of space, x stands for a length, ρ for a density, v for a velocity, and J and $\dot{w}$ are the diffusion and mass production source terms. In order to nondimensionalize that equation, each term needs to be expressed as a function of the basic flow properties. The boundary layer is not considered in the present study, diffusion is thus assumed to be negligible relative to the other terms and only the gas-phase chemistry is considered.

If only binary reactions are taken into account, Equation 1 is nondimensionalized as follows:

$$\partial \left(\overline{\rho}\overline{v_i}\right) / \partial \overline{x_i} = \rho \delta k_f A / v \quad (2)$$

where k_f is the forward reaction rate, δ is the shock stand-off, which is the characteristic length-scale of the region of interest, and A is a term that only depends on the species molar fraction and has the dimensions mol/kg. The group on the right-hand side of Equation 2 is a nondimensional number, that can be identified as a Damkhöler number Da. For a gas only composed of one species Y_2 and its dissociated counterpart Y, the only reaction is:

$$Y_2 + M \underset{k_b}{\overset{k_f}{\rightleftharpoons}} 2Y + M \quad (3)$$

where the collision partner M is either Y or Y_2. The constant A is then defined as:

$$A = \left(1 - \alpha^2\right) / 2M_m \quad (4)$$

where α is the mass fraction of dissociated gas, and M_m its molar mass.

In order to duplicate Da in the nonequilibrium layer, and thereby obtain the same solution to Equation 1, it is thus required that:

1. The test model has to have the same geometry and angle of attack as the hypersonic vehicle, and the test flow has to be the same mixture as the flow encountered in flight;
2. The product ρL and the specific free-stream enthalpy H_∞ have to be duplicated.
3. The Mach number is large enough (above $M_\infty \approx 4-6$) to apply the Oswatitsch Mach number independence principle [15]. Duplication of the Reynolds number is obtained through duplication of the product ρL.

The X2 Expansion Tube

General Procedure

The X2 expansion tube at The University of Queensland has been used to study planetary re-entry into the atmospheres of Earth, Mars, Venus, Titan, and the gas giants. It is composed of a reservoir, a driver, a shock tube, an acceleration tube, and can be operated with a Mach 10 nozzle. More details can be found in Gildfind [6].

To characterize the test flow, the test section is equipped with a rake of 9 pressure transducers each of them shielded by a 15 deg nose cone. The tips of the cones were positioned 10 ± 2 mm downstream of the nozzle exit plane. The axis of the cones are separated from each other by a vertical distance of 17.5 mm, spanning a total diameter of 140 mm. The axis of the central cone was aligned with the centerline of the core flow with an accuracy of ± 5 mm.

Experiments are recorded with a high-speed camera able to record 100 frames, at a rate of 1 µs per frame. The traces from the PCB transducers allows identifying what part of the flow corresponds to the passage of the test gas, which can be confirmed with the high-speed video if necessary. The signals from all the PCB transducers are then averaged during that period of time.

The increase in luminosity due to shock arrival is captured by a photodiode directed at the test section at an angle. This signal is used as the trigger for the data recording systems. Upon trigger, both the pressure transducers and the camera record data, including a set of pre-trigger samples (the data is cycled in a buffer and can be recorded for a certain amount of time).

The post-processing is done using *Pitot*, a one-dimensional equilibrium expansion tube simulator [11]. The fill pressures and the shock velocity in the different sections of the tube are specified in Pitot, and the nozzle area ratio is then varied until the total pressure measured by the cone probe transducers in the test flow is matched. The velocity of the flow entering the nozzle is assumed to be equal to that of the normal shock [14].

Once all the test gas properties are known, the free-stream enthalpy is computed as:

$$H_\infty^{\text{tot}} = v_\infty^2/2 + \int_{298\text{K}}^{T_\infty} c_p dT + \alpha E_d \quad (5)$$

where c_p is the heat capacity at constant pressure, and E_d is the enthalpy of formation of the dissociated products.

Varying Free-Stream Density while Maintaining Enthalpy

The objective of this study was to design flows with different free-stream density ρ_∞ but constant free-stream enthalpy H_∞. Therefore, if the dimensions of the test model are scaled so as to keep the product $\rho_\infty L$ constant, the flows should be similar from the binary scaling point of view.

The strategy adopted to produce such flows is to use steel plates of different thicknesses for the diaphragm separating the driver from the shock tube. The corresponding reservoir and driver fill conditions used were developed by by Gildfind during driver commissioning [6]. The parameters are tabulated in table 1.

Plate thickness [mm]	Reservoir pressure [MPa]	Driver pressure [kPa]	Burst pressure [MPa]	Relative burst pressure ratio [%]
1.2	4.95	110.3	15.5	43.4
2.0	6.85	92.8	27.9	78.2
2.5	6.10	77.2	35.7	100.0

Table 1: Change of operating conditions depending on primary diaphragm thickness. For this test campaign, the reservoir was filled with air and the driver with helium. Adapted from [6].

An ideal gas analytical solution of the flow processes along the tube show that the test gas properties depend on the pressure ratios across its different sections [18]. By scaling the pressure in the different sections of the tube by a factor equal to the burst ratio (see table 1), one can therefore retrieve the same free-stream enthalpy but a scaled pressure. This simplified approach gives a reasonable first approximation of the fill pressure required.

Design of Test Conditions in the X2 Expansion Tube

Experimental Campaign

The test gas of interest is a mixture of 97% CO_2 and 3% N_2, which corresponds to the high altitude atmosphere of Venus, and is close to that of Mars.

An initial estimate of the fill pressures needed to achieve a certain test flow condition is determined using L1D, a code originally developed by P. Jacobs [10]. It is a quasi-one-dimensional Lagrangian solver, with engineering correlations for viscous effects and point-mass dynamics for piston motions. The operating conditions were further refined during the experimental campaign.

The final conditions are detailed in table 2 for the operating conditions and table 3 for the resulting test flow. The data points obtained during the experimental campaign are also depicted in figure 2. Two sets were designed; set B does not include the 1.2 mm diaphragm as it would have resulted in a too rarefied flow. The standard deviation on the free-stream enthalpy is $\sigma = 1.6\%$ for set A and 4.4% for set B.

The flow obtained with the 2.5 mm diaphragm was chosen as reference case it had in the smallest standard deviation on free-stream density, allowing to determine the scale factors with a greater accuracy. The scale factors, defined as $K = L/L_{\text{mod}} = \rho_{\text{mod}}/\rho < 1$, are thus as summarized in the last column of table 3: 1.00 for the 2.5 mm plate, 0.50 for the 2.0 mm plate, and 0.17 for the 1.2 mm plate.

Numerical Investigations

The expected test flows were simulated with the Post-SHock relAXation solver (Poshax). Only set A was considered at this stage. Poshax, originally developed by Gollan [3], solves the one-dimensional variations of the inviscid flow properties behind a normal shock. The free-stream conditions are as specified in table 3, assuming equilibrium. A total of 15 species were included; CO_2, CO, CO^+, O_2, N_2, NO, CN, C_2, C, C^+, N, N^+, O, O^+, and e^-, with two temperatures. The Arrhenius reaction rates were taken from Ramjaun [17]. The energy exchange mechanisms were taken from Gnoffo [7] and Park [16]. Radiation coupling was not considered.

Set	Plate thickness [mm]	Test flow enthalpy [MJ/kg]	Test flow density [g/m^3]	Test flow temperature [K]	Normalized density [%]
A	1.2 ($N=3$)	42.67 ± 0.51	1.68 ± 0.23	2384 ± 25	16.9 ± 1.4
	2.0 ($N=3$)	45.99 ± 1.21	5.02 ± 0.18	2746 ± 20	50.5 ± 1.3
	2.5 ($N=3$)	42.42 ± 1.07	9.94 ± 0.68	2957 ± 40	100.0 ± 0.9
B	2.0 ($N=2$)	51.57 ± 0.18	3.04 ± 0.30	2654 ± 50	49.7 ± 3.6
	2.5 ($N=2$)	50.20 ± 0.07	6.13 ± 0.19	2852 ± 16	100.0 ± 0.2

Table 3: Free-stream conditions H_∞, ρ_∞, and T_∞ obtained for the operating conditions specified in tables 1 and 2.

Set	Plate thickness [mm]	Shock tube pressure [kPa]	Acc. tube pressure [Pa]
A	1.2	1.8	2
	2.0	3.6	40
	2.5	4.6	100
B	2.0	3.6	15
	2.5	4.6	39

Table 2: Fill pressure in the shock tube (97% CO_2 and 3% N_2), and in the acceleration tube (air). The diaphragm separating the shock tube from the acceleration tube is a single sheet of aluminum foil. The rest of the tube is as specified in table 1.

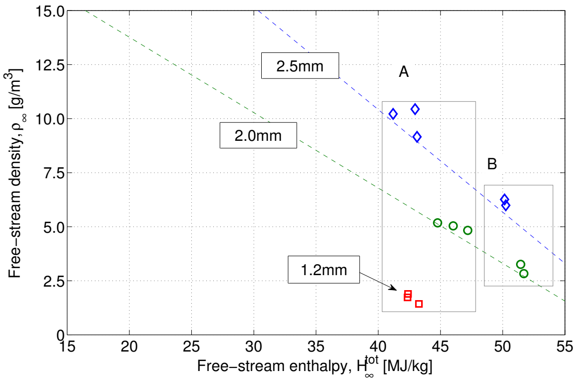

Figure 2: Data points obtained during the experimental campaign; ρ_∞ vs. H_∞. The two rectangles correspond to the two sets of flow conditions.

The results are depicted in figure 3 (a) for temperature (vibrational T_v and electronic T_e), (b) for scaled density, and (c) for mass fraction of CO, C, and O. In each plot, the normal distance from the shock was scaled according to the relative density in table 3: $x' = Kx$. The density in figure 3 (b) was divided by the same scale factor: $\rho' = \rho/K$. Despite small differences in free-stream enthalpy, all the scaled profiles match reasonably well.

With the scale factor defined as it is for this study, the density is smaller in the scaled shock layer while, ideally, its temperature is duplicated. For the same simplified gas described in Equation 3, the equilibrium constant K_c can be expressed as:

$$K_c(T) = \frac{\rho\alpha(T)^2}{2(1-\alpha(T))} M_m \tag{6}$$

If the density decreases, the fraction of dissociated gas increases accordingly so as to maintain a constant value of K_c, which only depends on temperature. Dissociation reactions being endothermic, however, that shift in concentration causes the scaled shock layer to be colder. A diminution in temperature in turn results in a smaller equilibrium constant, hindering dissociation, and a smaller density, favoring dissociation. The net effect on scaled shock layers with respect to the original one is a shift of concentration towards the products of dominating binary reactions (more dissociation or ionization), and a colder temperature.

This is indeed what is observed in figure 3 (a) and (c); the smaller the scale factor is, the colder is the shock layer and the more important is dissociation of CO into C and O. The lower concentration of C for the 1.2 mm case is due to a higher concentration of ionized C. The hotter shock layer for the 2.0 mm case the shock layer is explained by a higher total enthalpy relative to the two other cases (see table 3).

From Equation 2, the scaling parameter to be used is $\rho\delta$, where ρ is the density in the shock layer. However, neither of those quantities are known prior to the experiment. It is therefore preferred to use the product $\rho_\infty R$, both being linked through experimental correlations such as that proposed by Van Dyke's [19]:

$$\rho\delta = 0.82 \cdot \rho_\infty R \tag{7}$$

where R is the model's nose radius. The mismatch in the scaled density in figure 3 (b) is because Van Dyke's correlation is only approximate; the product $\rho_\infty R$ is not exactly a linear function of $\rho\delta$.

The equilibrium concentrations were included as symbols in figure 3 (c). Those were obtained with Chemical Equilibrium with Applications (CEA), a software tool developed at the NASA Lewis Research Centre [13] which provides equilibrium flow properties for any given pressure and temperature. The flow appears to be frozen, indicating a small forward reaction rate constant (Equation 2).

Conclusions

Binary scaling is a similitude law used in high-enthalpy facilities dedicated to the study of hypersonic blunt bodies. It requires duplication of the product of density and a length scale of the flow, ρL, as well as the free-stream enthalpy H_∞^{tot}. Experiments are thus performed at densities higher than in those encountered in flight. This is known to have an effect on equilibrium composition, nonequilibrium thermal kinetic processes, and higher order reaction (ternary, etc.) rates when they become significant. The effect of these processes on the overall development of radiating shock layers has not been comprehensively investigates yet.

Flow conditions of different free-stream density ρ_∞ but almost constant free-stream enthalpy were designed for the X2 super-orbital expansion tube. It was demonstrated with numerical simulations that the match between the scaled temperature, density, and concentration profiles was satisfying, despite small variations in free-stream temperature and enthalpy.

Those conditions will be used to compare the shock layers forming in front of models of different size, but similar from the

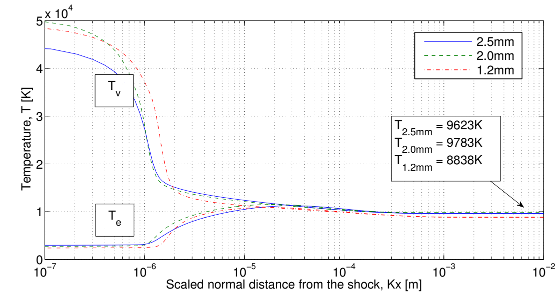

(a)

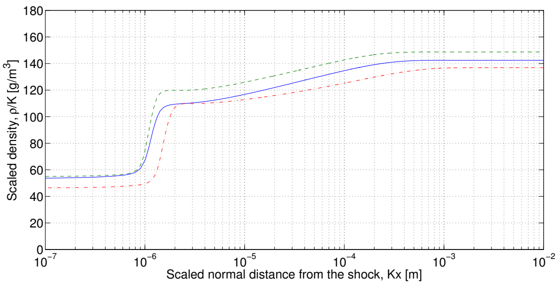

(b)

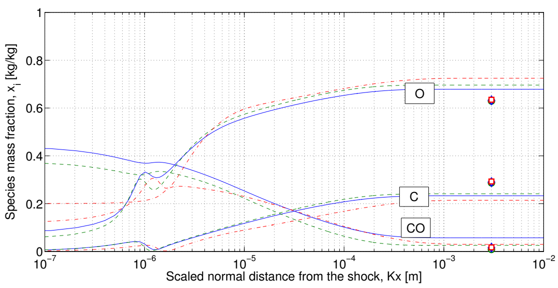

(c)

Figure 3: Evolution of the temperature (a), scaled density (b), and concentration of O, C and CO (c) downstream of a normal shock in the test flow conditions as described in table 3. Those results were obtained with Poshax. The symbols in figure (c) correspond to the equilibrium concentrations. The scale factors K are 1.00 for the 2.5 mm plate, 0.505 for the 2.0 mm plate, and 0.169 for the 1.2 mm plate.

binary scaling point of view. The results from that future test campaign will provide useful data both for the accuracy of binary scaling, and for the aerothermochemical processes of high enthalpy $CO_2 - N_2$ mixtures.

Acknowledgements

The authors would like to thank the operators of the X2: H. Wei, B. Wheatley, and particularly E. Fahy, C. James and S. Lewis who put a great amount of effort into this campaign.

References

[1] Birkhoff, M., *Hydrodynamics. A study in Logic, Fact, and Similitude*, Princeton University Press, 1951.

[2] Ellington, D., Binary Scaling Limits for Hypersonic Flight, *AIAA J.*, **5(9)**, September 1967, 1705–1706.

[3] Gollan, R.J. and Jacobs, P.A., About the Formulation, Verification and Validation of the Hypersonic Flow Solver Eilmer, *Int. J. Numer. Meth. Fluids.*, **73**, 2013, 19–57.

[4] Gibson, W.E., Dissociation Scaling for Nonequilibrium Blunt-Nose Flows, *American Rocket Society J.*, **32(2)**, February 1962, 285.

[5] Gibson, W.E. and Marrone, P.V., A Similitude for Nonequilibrium Phenomena in Hypersonic Flight, in *AGARD Meeting on High Temperature Aspects of Hypersonic Fluid Dynamics*, editor W. Nelson, Oxford, April 1962.

[6] Gildfind, D., *Development of High Total Pressure Scramjet Flow Conditions Using the X2 Expansion Tube*, PhD thesis, University of Queensland, 2012.

[7] Gnoffo, P.A., Gupta, R.N. and Shinn, J. L., *Conservation Equations and Physical Models for Hypersonic Air Flows in Thermal and Chemical Nonequilibrium*, Technical Report 2867, NASA, 1989.

[8] Hall, J.G., Eschenroeder, A. Q. and Marrone, P. V., Blunt-Nose Inviscid Airflows With Coupled Nonequilibrium Processes, *J. Aerosp. Sci.*, **29(9)**, 1962, 1038–1051.

[9] Hornung, H.G., Experimental Real-Gas Hypersonics, *Aeronaut. J.*, **92**, 1988, 379–389.

[10] Jacobs, P.A., Quasi-One-Dimensional Modelling of a Free-Piston Shock Tunnel, *AIAA J.*, **32(1)**, 1994, 137–145.

[11] James, C., Gildfind, D., Morgan, R.G., Jacobs, P.A. and Zander, F., Designing and Simulating High Enthalpy Expansion Tube Conditions, in *Proceedings of the 2013 Asia-Pacific International Symposium on Aerospace Technology*, November 2013.

[12] Lu, F.K. and Marren, D.E., Principles of Hypersonic Test Facility Development, in *Advances Hypersonic Test Facilities, Progress in Astronautics and Aeronautics*, editor P. Zarchan, AIAA, New York, 1994, 17–25.

[13] McBride, D. and Gordan, G., *Computer Program for Calculations of Complex Chemical Equilibrium and Applications II, Users Manual and Program Description*, Technical Report RP-1311-P2, NASA, 1996.

[14] Mirels, H., Shock Tube Test Time Limitation due to Turbulent-Wall Boundary Layer, *AIAA J.*, **2(1)**, January 1963, 84–93.

[15] Oswatitsch, K., *Contributions to the Development of Gas Dynamics*, chapter Laws of Similarity and Equivalence, Vieweg, 1980.

[16] Park, J., Howe, J., Jaffe, R. and Candler, G., Review of Chemical-Kinetic Problems of Future NASA Missions, II: Mars Entries, *J. Thermophys. Heat Tr.*, **8(1)**, 1994, 9–22.

[17] Ramjaun, D., TC2: Definition of Shock Tunnel Test Cases for Gas Radiation Prediction in a Planetary Atmosphere, in *Proceedings of the International Workshop on Radiation of High Temperature Gases in Atmospheric Entry*, ESA SP-533, October 2003.

[18] Trimpi, R.L., *A Preliminary Theoretical Study of the Expansion Tube, a New Device for Producing High-Enthalpy Short-Duration Hypersonic Gas Flows*, Technical Report R-133, NASA, 1962.

[19] Van Dyke, M.D., The Supersonic Blunt-Body Problem Review and Extension, *J. Aeronaut. Sci.*, **25**, 1958, 485-495.